A Letters Journal Exploring the Frontiers of Physics

October 2022

EPL, **140** (2022) 10001
doi: 10.1209/0295-5075/ac932f

www.epljournal.org

Four-channel parity-time symmetry

Ege Özgün[1(a)], Ekmel Ozbay[2,3] and Ibrahim Ozdur[4]

[1] *Department of Physics Engineering, Hacettepe University, Beytepe - 06800 Ankara, Turkey*
[2] *NANOTAM-Nanotechnology Research Center, Bilkent University - 06800 Ankara, Turkey*
[3] *Department of Physics, Department of Electrical and Electronics Engineering and UNAM-Institute of Materials Science and Nanotechnology, Bilkent University - 06800 Ankara, Turkey*
[4] *Electrical and Electronics Engineering Department, TOBB University of Economics and Technology 06560, Ankara, Turkey*

received 3 May 2022; accepted in final form 20 September 2022
published online 27 September 2022

Abstract – In this letter, we propose a general scheme for four-channel parity-time symmetry. We theoretically demonstrate how to achieve novel features via exploiting the parity-time symmetry for four-channel coupled-mode equations and study the spontaneous symmetry breaking manifold, separating the parity-time symmetric and parity-time broken regimes, for various parameter configurations. We also propose a possible candidate (an optoelectronic oscillator) which can demonstrate the theoretically derived features, which include broadband tunability, eigenfrequency selection and flipping, and single/dual frequency operation regimes.

Recently, the concept of spontaneous symmetry breaking (SSB) from quantum field theories has been adopted in an ingenious way for the case of parity time ($\mathcal{PT}$) symmetry-breaking in optical systems. The concept of $\mathcal{PT}$-symmetry was initially introduced within the context of quantum mechanics, which flexes the condition of a quantum mechanical Hamiltonian to be $\mathcal{PT}$-symmetric instead of being Hermitian. Hermiticity guarantees a real energy spectra and the unitary evolution of the states which are the fundamental postulates of a quantum theory. However, in the late nineties, Bender and Boettcher showed that those fundamental principles of quantum mechanics can also be satisfied with $\mathcal{PT}$-symmetric Hamiltonians at least for a certain range of parameters [1,2]. Pseudo-Hermiticity is then introduced by Mostafazadeh, stating that every Hamiltonian with real spectra is pseudo-Hermitian and that $\mathcal{PT}$-symmetric Hamiltonians belong to that class [3]. The concept of $\mathcal{PT}$-symmetry is then borrowed in the fields of optics and photonics [4–15]. The principle idea behind adopting $\mathcal{PT}$-symmetry in these fields relies on engineering platforms with equal gain/loss (GL) which was realized in the aforementioned studies in numerous different ways. Those gave rise to $\mathcal{PT}$-symmetric structures, displaying prominent phenomena including, but not limited to, lasing, uni-directional invisibility and anisotropic transmission resonances. $\mathcal{PT}$-symmetry is also studied for the scattering problem with polarization dependence in photonics [16] and for spin-$\frac{1}{2}$ particles in quantum mechanics [17].

Optoelectronic oscillators (OEOs) are devices that are capable of producing stable and low phase noise single microwave modes [18,19]. The main challenge in OEOs is to maintain single-mode oscillation while further decreasing the phase noise via longer delay lines and high Q bandpass filters. Different schemes such as dual loop [20,21] and high Q optical filter [22,23] were proposed to overcome this problem. The same motivation used in $\mathcal{PT}$-optics studies of equal GL is recently applied to OEOs to overcome the single mode selectivity/long delay line (low phase noise) dilemma [24]. This is achieved via forcing an equal GL $\mathcal{PT}$-symmetric system to go under SSB. A multitude of studies followed the first $\mathcal{PT}$-OEO demonstration: A $\mathcal{PT}$-OEO based on dual wavelength carriers in a single loop configuration [25], tunable $\mathcal{PT}$-OEOs based on dual-parallel Mach-Zehnder modulator [26], based on laser wavelength tuning [27], based on a microdisk resonator [28], based on a microwave photonic filter [29], a polarization-dependent Sagnac loop [30] and polarization multiplexing [31] are among those.

In this work, we propose a general scheme for realizing four-channel $\mathcal{PT}$-symmetry, and theoretically study the SSB manifold, which separates the $\mathcal{PT}$-symmetric and $\mathcal{PT}$-broken configurations. We will first derive the eigenfrequency spectrum for the four-channel case, starting

(a) E-mail: egeozgun@hacettepe.edu.tr (corresponding author)

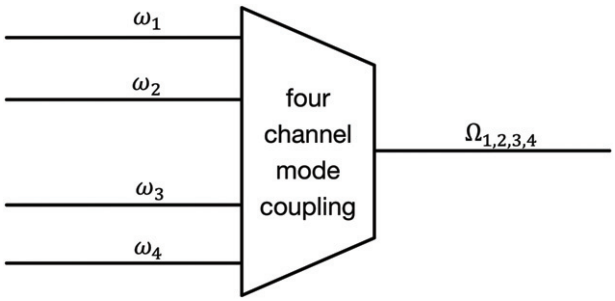

Fig. 1: The generic scheme for four-channel mode coupling. ω_i and Ω_i denote the individual frequencies in channels before the coupling and the eigenfrequencies of the system after mode coupling, respectively, for $(i = 1, 2, 3, 4)$.

from the coupled-mode formalism. Then we will investigate different features of the derived eigenfrequency set and analyze $\mathcal{PT}$-symmetric and $\mathcal{PT}$-broken regions of the spectrum separated by the SSB manifold. Then we conclude by suggesting a possible platform of OEO in which our theoretical results can be implemented.

For the general scheme we depict in fig. 1, the coupled-mode equations describing the four-channel mixing can be cast as

$$-i\dot{c}_1 = \omega_1 c_1 - ig_t + \kappa_{12}c_2 + \kappa_{13}c_3 + \kappa_{14}c_4, \quad (1a)$$

$$-i\dot{c}_2 = \omega_2 c_2 + il_t + \kappa_{21}c_1 + \kappa_{23}c_3 + \kappa_{24}c_4, \quad (1b)$$

$$-i\dot{c}_3 = \omega_3 c_3 - ig_b + \kappa_{31}c_1 + \kappa_{32}c_2 + \kappa_{34}c_4, \quad (1c)$$

$$-i\dot{c}_4 = \omega_4 c_4 + il_b + \kappa_{41}c_1 + \kappa_{42}c_2 + \kappa_{43}c_3, \quad (1d)$$

where dot denotes time derivative, c_σ are the amplitudes at different channels, ω_σ are the frequencies prior to coupling with $\sigma = [1, 2, 3, 4]$, g_η and l_η, with $\eta = [t, b]$ are gain and loss amplitudes in top $(1, 2)$ and bottom $(3, 4)$ channels, respectively, and finally κ_{jk} with $(j \neq k) = [1, 2, 3, 4]$ is the coupling coefficient between the channels j and k. It is important to note that all terms in the above equations and in all other equations that will follow are mode-dependent and mode indices are dropped out for the sake of a more compact notation. For obtaining the desired four-channel $\mathcal{PT}$-symmetry, some conditions need to be satisfied: Firstly, gain and loss amplitudes in respective top and bottom channels must be equal, *i.e.*, $g_t = l_t$ and $g_b = l_b$, which are required for $\mathcal{PT}$-symmetric configurations. Assuming channels with identical properties, we can also take ω_σ's to be equal, which we now simply call ω. Secondly, we require the gain and loss in opposing top and bottom channels to be also equal, $g_t = g_b \equiv \gamma$. Finally we want i) equal coupling coefficients for coupling between respective top $(1, 2)$ and bottom $(3, 4)$ channels, ii) equal coupling coefficients between top and bottom channels. These two restrictions give the following conditions on the coupling coefficients: $\kappa_{12} = \kappa_{34} \equiv \kappa_1$ and $\kappa_{13} = \kappa_{14} = \kappa_{23} = \kappa_{24} \equiv \kappa_2$. Here the complex κ_1 can also be expressed as its magnitude $|\kappa_1|$ and its phase ϕ as $\kappa_1 = |\kappa_1|e^{i\phi}$, which will be important when we start to talk about the different features of the platform suggested. Also using the fact that $\kappa_{jk} = \kappa_{kj}^*$ we can recast the coupled mode equations as $\det\left[\mathbb{M} - \Omega\mathbb{1}\right] = 0$ with

$$\mathbb{M} = \begin{pmatrix} \omega + i\gamma & \kappa_1 & \kappa_2 & \kappa_2 \\ \kappa_1^* & \omega - i\gamma & \kappa_2 & \kappa_2 \\ \kappa_2^* & \kappa_2^* & \omega + i\gamma & \kappa_1 \\ \kappa_2^* & \kappa_2^* & \kappa_1^* & \omega - i\gamma \end{pmatrix}, \quad (2)$$

where $\mathbb{1}$ is the four-by-four unit matrix and Ω are the eigenfrequencies of our system. Solving $\det\left[\mathbb{M} - \Omega\mathbb{1}\right] = 0$, we obtain the eigenspectrum of the system as

$$\begin{aligned} \Omega_{1,2} &= \omega + |\kappa_2| \pm \sqrt{\left[S_+\right]^2 - \gamma^2}, \\ \Omega_{3,4} &= \omega - |\kappa_2| \pm \sqrt{\left[S_-\right]^2 - \gamma^2}, \\ S_\pm &= \sqrt{|\kappa_1|^2 + |\kappa_2|^2 \pm 2\Re[\kappa_1]|\kappa_2|}. \end{aligned} \quad (3)$$

Here, $\Re[\kappa_1]$ denotes the real part of κ_1. Equations (3) offer us a vast selection of applications.

Let us define new parameters, $F_\pm \equiv [S_\pm]^2 - \gamma^2$, which will serve as a direct measure of SSB. When $F_+ > 0$ and $F_- > 0$ the platform is operating at the $\mathcal{PT}$-symmetric regime thus has neutral eigenspectrum. When any of $F_\pm = 0$, SSB onsets and for $F_\pm < 0$ we reach the $\mathcal{PT}$-broken regime where the eigenspectrum becomes complex, giving rise to oscillating eigenspectra. Parameter ranges for achieving $\mathcal{PT}$-transition, *i.e.*, the SSB manifolds, $F_\pm = 0$ for the two eigenfrequency sets at fixed γ (fig. 2) and at fixed ϕ (fig. 3) are shown. Moreover, as a measure of $\mathcal{PT}$-symmetry, $F_\pm$ are plotted *vs.* γ and ϕ at fixed $|\kappa_1| = |\kappa_2| = 3$ in fig. 4.

We are now in a position to talk about the different features offered by this suggested scheme. The first application is achieving single mode oscillation, realized when one of the two conditions below is satisfied:

$$S_- < \gamma < S_+ \qquad \text{or} \qquad S_+ < \gamma < S_-. \quad (4)$$

The term $\Re[\kappa_1]$ poses great importance in the above inequality. We can re-write it as $|\kappa_1|\cos(\phi)$, where ϕ for

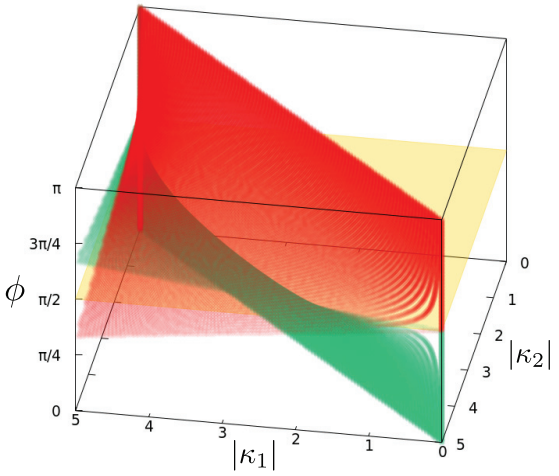

Fig. 2: SSB manifold, $F_+(|\kappa_1|, |\kappa_2|, \phi) = 0$ (green) and $F_-(|\kappa_1|, |\kappa_2|, \phi) = 0$ (red) plotted for fixed GL, $\gamma = 5$. All values are given in dimensionless form. Since they all have the same dimensionality the scaling is invariant. The parameter range for breaking $\mathcal{PT}$-symmetry at fixed γ via tuning κ_1, κ_2 and ϕ is displayed. $\phi = \pi/2$ surface is illustrated in yellow.

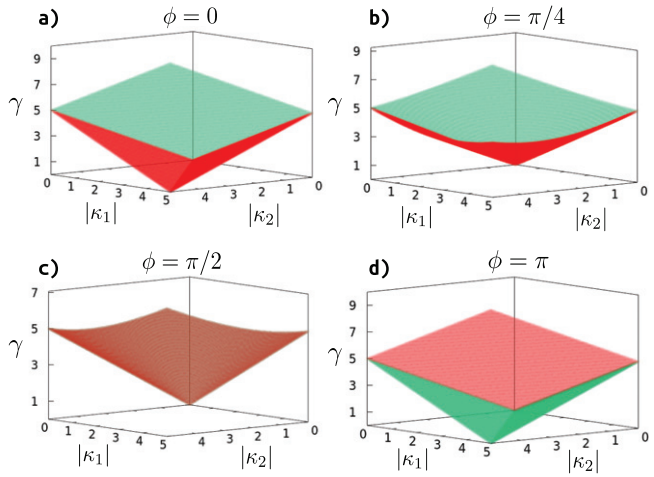

Fig. 3: SSB manifold, $F_+(|\kappa_1|, |\kappa_2|, \gamma) = 0$ (green) and $F_-(|\kappa_1|, |\kappa_2|, \gamma) = 0$ (red) plotted at fixed ϕ again in dimensionless form, for (a) $\phi = 0$, (b) $\phi = \pi/4$, (c) $\phi = \pi/2$ at which two manifolds exactly match, and (d) $\phi = \pi$. Eigenspectrum switching for ϕ: $0 \to \pi$ and achieving SSB for various values of $|\kappa_1|$,$|\kappa_2|$ and γ are illustrated.

instance for the case of an OEO is the phase difference between the electric field components at different channels. Hence, we can directly switch between the two sets of eigenfrequencies $\Omega_{1,2}$ and $\Omega_{3,4}$, which means we can change our oscillating frequency from $\omega + |\kappa_2|$ to $\omega - |\kappa_2|$ just by changing ϕ from 0 to π. Moreover, for a fixed GL amplitude γ, by changing ϕ, single mode oscillation condition depicted in eq. (4) can also be obtained.

Another novel feature that our platform offers is the possibility to tune the oscillating frequency by changing the coupling constant $|\kappa_2|$. For the suggested scheme, $|\kappa_2|$

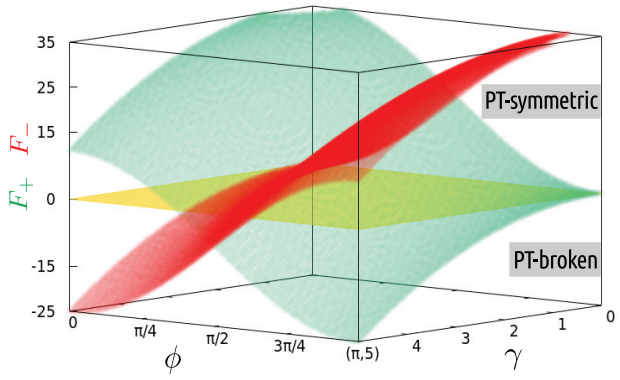

Fig. 4: The measure of $\mathcal{PT}$-symmetry for our platform, $F_\pm$ plotted at fixed $|\kappa_1| = |\kappa_2| = 3$ (once more in dimensionless form) for varying γ and ϕ. When F_+ and F_- are both positive, our platform is in the $\mathcal{PT}$-symmetric phase whereas, when either of $F_\pm$ is less than zero, the $\mathcal{PT}$-broken phase onsets.

can theoretically be tuned up to a maximum value of $\omega/2$, thus giving a broadband frequency selectivity $\omega \pm \frac{1}{2}\Delta\Omega$, with $\Delta\Omega = 2|\kappa_2|$. For instance an oscillating mode with a 10 GHz frequency will have a wideband selectivity between 5 GHz and 15 GHz.

There is a great variety of both theoretical and experimental studies on achieving tunable coupling coefficients [32–37] for the optical as well as the RF regime. To reflect the potential of our proposal in a more substantial manner, we will briefly discuss the theoretical upper bound for the tuning capability of the suggested scheme with a simple mathematical formulation. We will present the formulation based on the coupling of fiber optic channels, nevertheless the conclusion is also valid for coupling in the RF regime. The coupling coefficient for any two channels can be given in a normalization-independent form as

$$\kappa_{jk} = \frac{\omega}{4} \frac{\int \mathrm{d}\sigma \; \delta\varepsilon \; \mathbf{E}_j \cdot \mathbf{E}_k^*}{\frac{1}{2} \int \mathrm{d}\sigma \; \varepsilon \; \mathbf{E}_j \cdot \mathbf{E}_j^*}, \tag{5}$$

where the area integral is performed over the cross-section of the channels, $\delta\varepsilon$ is the deviation of dielectric index from the surrounding medium ε and $\mathbf{E}$ denotes the electric field vectors at respective channels. When the electric field strengths are equal, which is valid for our scheme, we can simplify eq. (5) in the following form assuming $\delta\varepsilon$ and ε are not position dependent:

$$\kappa_{jk} = \frac{\omega}{2} \frac{\delta\varepsilon}{\varepsilon} e^{i\phi_{jk}}. \tag{6}$$

The magnitude of the coupling coefficient is independent of the relative phase ϕ_{jk} between the electric fields, whereas the real part depends on the phase:

$$|\kappa_{jk}| = \frac{\omega}{2} \frac{\delta\varepsilon}{\varepsilon}, \qquad \Re[\kappa_{jk}] = \frac{\omega}{2} \frac{\delta\varepsilon}{\varepsilon} \cos(\phi_{jk}). \tag{7}$$

The term $\delta\varepsilon/\varepsilon$ cannot exceed unity, thus it sets a theoretical limit for the coupling coefficient as $|\kappa_{jk}| \lesssim \omega/2$.

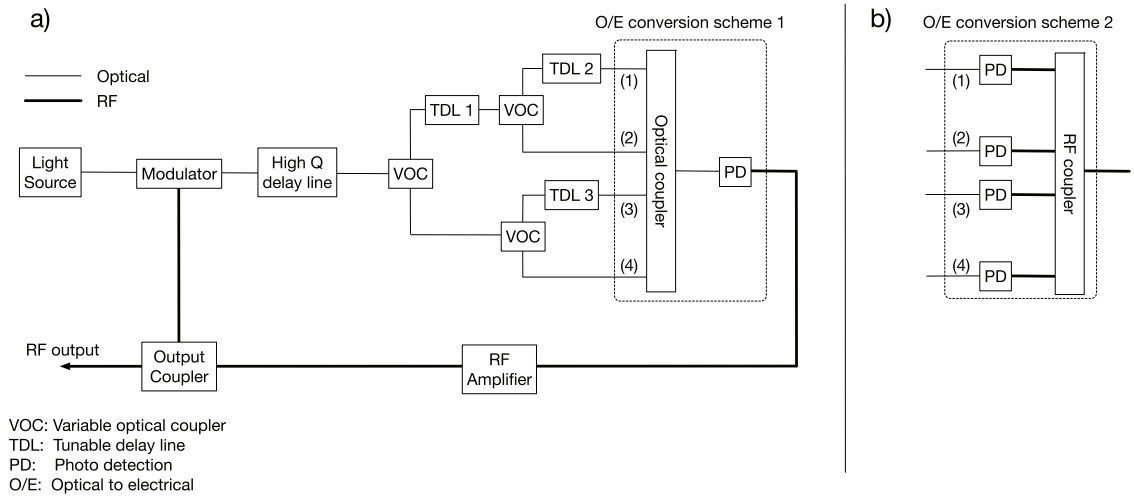

Fig. 5: Block diagram of a possible implementation of our suggested scheme as an OEO with two different configurations. (a) Optical coupling; (b) RF coupling.

The final novelty offered by our platform is the dual frequency operation regime. This is achieved when one of the below conditions is satisfied:

$$S_- \leq S_+ < \gamma \qquad \text{or} \qquad S_+ \leq S_- < \gamma. \tag{8}$$

The easiest way to achieve this is by setting $\phi = \pi/2$ when $|\kappa_1|^2 + |\kappa_2|^2 < \gamma$. This configuration gives a dual frequency oscillation with $\Delta\Omega = 2|\kappa_2|$. As shown above, theoretically $|\kappa_2|$ can take a maximum value of $\omega/2$, therefore we can have dual frequency oscillation, with the two frequencies separated as large as the original frequency ω. The dual frequency operation regime can also be invoked by tuning γ.

As a possible implementation of the above-mentioned features, we briefly talk about the case for an OEO. Figure 5 displays a possible platform design to achieve the features discussed above. In the suggested platform (fig. 5(a)) the optoelectronic loop starts with a continuous wave light generated from the light source, then it is fed into the modulator. Next it enters into a single mode high-Q optical delay line. After that, the signal is separated into two channels via the variable optical coupler (VOC). It is also possible to use a polarization beam splitter combined with a polarization controller for the same purpose. Then it passes through TDL1 in one channel to balance the phases in two channels, prior to four-channel separation. Then both channels are further separated into two via the VOCs again, creating the quadruple loop. One of the two channels at the top and bottom has a TDL. Those TDLs, to be specific, TDL2 and TDL3, can be tuned synchronously to obtain eigenspectrum switching and also breaking of $\mathcal{PT}$-symmetry. Afterwards, the four channels are brought together at a combiner that allows tunable coupling coefficients at optical regime. Then the signal is converted to RF via the photodetector, fed into an electrical amplifier and split into two. One path is the RF-output for analyses, whereas the other is fed back into the modulator to complete the loops. An alternative design for coupling the channels in the RF regime instead of the optical regime is also illustrated in fig. 5(b).

It is important to mention the exceptional points in connection with the suggested platform. The exceptional points in the OEO system suggested correspond to the sets of parameters that separate the $\mathcal{PT}$-symmetric and $\mathcal{PT}$-broken phases of the system. In other words, the collection of exceptional points form the SSB manifold, plotted in figs. 2, 3 and 4. All these exceptional points correspond to the onset of interesting phenomena, *i.e.*, the features of the platform we described above in detail, namely broadband tunability, eigenfrequency selection and flipping, and single/dual frequency operation regimes. To obtain these features, each time only one of the parameters is continuously changed, whereas the remaining parameters are fixed, so that from the SSB manifold, each of these selections corresponds to a single point, which are the exceptional points.

Before concluding it would be useful to make a brief comparison of the suggested scheme's possible $\mathcal{PT}$-OEO implementation with other $\mathcal{PT}$-OEOs. Firstly, our platform would enjoy the same advantage of large gain difference between successive modes, thanks to the square root structure of $F_\pm$, hence does not require a band-pass filter for mode selection. This means, it would also share the same low phase noise feature of other $\mathcal{PT}$-OEOs since we can choose a longer optical delay line without being limited by the resolution of the band-pass filter. On the other hand, our scheme would offer enhanced and novel features of tunabilty via the coupling coefficient, eigenspectrum switching, single/dual frequency operation and $\mathcal{PT}$-breaking via phase, coupling coefficient and GL amplitude tuning.

To sum up, we suggested a multi-functional four-channel scheme that relies on $\mathcal{PT}$-symmetry, which allows frequency tunability, with single and dual frequency operation options in a single platform. We theoretically

studied the SSB manifold and $\mathcal{PT}$-symmetric and $\mathcal{PT}$-broken regimes for sets of different parameters. Our suggested scheme brings four applications: i) Flexibility of breaking the $\mathcal{PT}$-symmetry via different parameters, *i.e.*, by tuning the coupling coefficient, GL amplitude or phase. ii) Eigenfrequency flipping, *i.e.*, direct switching between the two well-separated sets of eigenfrequencies by tuning the phase. iii) Frequency selection by tuning the coupling coefficient between top/down channels $|\kappa_2|$. iv) Dual frequency operation regime with a frequency separation up to a theoretical maximum of the original frequency ω. We believe that our proposal is promising for numerous device applications thanks to its versatility.

* * *

This work is partially supported by the Turkish Academy of Sciences (TUBA) and The Young Scientists Award Programme 2018 granted by TUBA (TUBA, GEBIP 2018).

Data availability statement: All data that support the findings of this study are included within the article (and any supplementary files).

REFERENCES

[1] Bender C. M. and Boettcher S., *Phys. Rev. Lett.*, **80** (1998) 5243.
[2] Bender C. M., Boettcher S. and Meisinger P. N., *J. Math. Phys.*, **40** (1999) 2201.
[3] Mostafazadeh A., *J. Math. Phys.*, **43** (2002) 205; 2814; 3944.
[4] El-Ganainy R., Makris K., Christodoulides D. and Musslimani Z. H., *Opt. Lett.*, **32** (2007) 2632.
[5] Musslimani Z., Makris K. G., El-Ganainy R. and Christodoulides D. N., *Phys. Rev. Lett.*, **100** (2008) 030402.
[6] Makris K. G., El-Ganainy R., Christodoulides D. and Musslimani Z. H., *Phys. Rev. Lett.*, **100** (2008) 103904.
[7] Klaiman S., Günther U. and Moiseyev N., *Phys. Rev. Lett.*, **101** (2008) 080402.
[8] Guo A., Salamo G., Duchesne D., Morandotti R., Volatier-Ravat M., Aimez V., Siviloglou G. and Christodoulides D., *Phys. Rev. Lett.*, **103** (2009) 093902.
[9] Makris K. G., El-Ganainy R., Christodoulides D. N. and Musslimani Z. H., *Phys. Rev. A*, **81** (2010) 063807.
[10] Rüter C. E., Makris K. G., El-Ganainy R., Christodoulides D. N., Segev M. and Kip D., *Nat. Phys.*, **6** (2010) 192.
[11] Ramezani H., Kottos T., El-Ganainy R. and Christodoulides D. N., *Phys. Rev. A*, **82** (2010) 043803.
[12] Feng L., Wong Z. J., Ma R.-M., Wang Y. and Zhang X., *Science*, **346** (2014) 972.
[13] Zhu X., Feng L., Zhang P., Yin X. and Zhang X., *Opt. Lett.*, **38** (2013) 2821.
[14] Sounas D. L., Fleury R. and Alù A., *Phys. Rev. Appl.*, **4** (2015) 014005.
[15] Lin Z., Ramezani H., Eichelkraut T., Kottos T., Cao H. and Christodoulides D. N., *Phys. Rev. Lett.*, **106** (2011) 213901.
[16] Özgün E., Serebryannikov A. E., Ozbay E. and Soukoulis C. M., *Sci. Rep.*, **7** (2017) 1.
[17] Özgün E., Hakioğlu T. and Ozbay E., *EPL*, **131** (2020) 11001.
[18] Yao X. S. and Maleki L., *IEEE J. Quantum Electron.*, **32** (1996) 1141.
[19] Tang J., Hao T., Li W., Domenech D., Baños R., Muñoz P., Zhu N., Capmany J. and Li M., *Opt. Express*, **26** (2018) 12257.
[20] Yao X. S. and Maleki L., *IEEE J. Quantum Electron.*, **36** (2000) 79.
[21] Shumakher E. and Eisenstein G., *IEEE Photon. Technol. Lett.*, **20** (2008) 1881.
[22] Ozdur I., Mandridis D., Hoghooghi N. and Delfyett P. J., *J. Lightwave Technol.*, **28** (2010) 3100.
[23] Li W. and Yao J., *IEEE Trans. Microw. Theory Tech.*, **60** (2012) 1735.
[24] Zhang J. and Yao J., *Sci. Adv.*, **4** (2018) eaar6782.
[25] Li L., Wang G., Zhang J. and Yao J., *2019 International Topical Meeting on Microwave Photonics (MWP)* (IEEE) 2019, pp. 1–4.
[26] Ding Q., Wang M., Zhang J., Mu H., Wang C. and Fan G., *J. Lightwave Technol.*, **38** (2020) 6569.
[27] Teng C., Zou X., Li P., Xie C., Sun Y., Pan W. and Yan L., *IEEE Photon. Technol. Lett.*, **32** (2019) 47.
[28] Fan Z., Zhang W., Qiu Q. and Yao J., *J. Lightwave Technol.*, **38** (2020) 2127.
[29] Li P., Dai Z., Fan Z., Yan L. and Yao J., *Opt. Lett.*, **45** (2020) 3139.
[30] Dai Z., Fan Z., Li P. and Yao J., *J. Lightwave Technol.*, **38** (2020) 5327.
[31] Özgün E., Uyar F., Kartaloglu T., Ozbay E. and Ozdur I., *J. Opt.*, **24** (2022) 055802.
[32] Digonnet M. J. and Shaw H. J., *IEEE Trans. Microw. Theory Tech.*, **30** (1982) 592.
[33] Haus H. A., *Waves and Fields in Optoelectronics* (Prentice-Hall) 1984.
[34] Haus H. A. and Huang W., *Proc. IEEE*, **79** (1991) 1505.
[35] Lehmann T., Mextorf H. and Knoechel R., in *2008 38th European Microwave Conference* (IEEE) 2008, pp. 199–202.
[36] Zhang T. and Che W., *IEEE Microw. Wireless Compon. Lett.*, **27** (2017) 129.
[37] Pan Y., Zheng S., Hong W. and Chan W. S., *IEEE Trans. Ind. Electron.*, **68** (2020) 2408.